

Temperature-dependent dispersion equations for KTiOPO_4 and KTiOAsO_4

Shai Emanuelli and Ady Arie

We have measured the thermal expansion and the temperature dependence of z and y components of the refractive index for KTiOPO_4 and KTiOAsO_4 , in the wavelength range 532–1585 nm and temperature range 25–200 °C, using an interferometric technique. The measurements were used to derive temperature-dependent Sellmeier equations for the two materials. These equations predict with good agreement the temperature dependence of quasi-phase-matched nonlinear frequency converters. © 2003 Optical Society of America

OCIS codes: 120.2230, 120.3180, 190.4400.

1. Introduction

Quasi-phase matching is widely used as an efficient and flexible method of nonlinear frequency conversion. In particular, it has been successfully implemented in KTiOPO_4 (KTP)¹ and its isomorphs [KTiOAsO_4 (KTA), RbTiOAsO_4 , etc.], where the periodic modulation of the nonlinear coefficient of the material can be achieved by electric field poling. To accurately design the poling period in nonlinear frequency mixers and predict their spectral and thermal characteristics, the dependence of the refractive index of the material on wavelength and temperature must be accurately known.

Although the wavelength dependence of refractive indices for materials from the KTP family is known with sufficient accuracy,^{1–3} there are discrepancies between the measured and the calculated results for various temperature-dependent nonlinear mixing devices. As an example, the temperature tuning of a periodically poled KTP (PPKTP) optical parametric oscillator (OPO)⁴ idler wavelength deviates from the theoretical predictions based on Wiechmann *et al.*⁵ and Kato⁶ by as much as 20 and 60 nm, respectively, at 200 °C. The recent work of Kato and Takaoka,⁷ which is based on several published nonlinear exper-

imental results, provides a better fit for KTP, but still shows deviations from the experimental results. The temperature-dependent tuning curve and the temperature FWHM of PPKTP and periodically poled KTA difference frequency generators^{1,2} are significantly different from the theoretical values. Furthermore, to the best of our knowledge, the temperature dependence of the KTA refractive index has not been measured nor published.

Owing to the increasing importance of KTP and its isomorphs in nonlinear optics, and the inaccurate or missing data for the temperature dependence, we report in this paper new measurements on the thermal dependence of the refractive index of KTP and KTA taken over a wide wavelength and temperature range. These measurements enabled us to derive new temperature dependent Sellmeier equations for the y and z directions in these two materials.

Our measurement technique was based on the simple fact that, owing to the Fresnel reflection from the uncoated crystal end faces, the crystal acts as a Fabry-Perot etalon. Varying the crystal temperature will change the optical path inside the crystal, thereby causing periodic change in the crystal transmission and reflection, which consequently will cause periodical change of light intensity that is transmitted or reflected from the crystal. The measurement of light intensity variation gives the optical path change variation inside the crystal as function of temperature. To derive the temperature-dependent change of the refractive index from such a measurement, one must subtract the contribution of the crystal length thermal expansion. Based on these simple ideas our experiment was divided into two parts: the measurement of the optical path change

The authors are with the Department of Electrical Engineering—Physical Electronics, Faculty of Engineering, Tel-Aviv University, Tel-Aviv 69978, Israel. S. Emanuelli's e-mail address is shai.emanuelli@hp.com.

Received 27 March 2003; revised manuscript received 17 July 2003.

0003-6935/03/336661-05\$15.00/0

© 2003 Optical Society of America

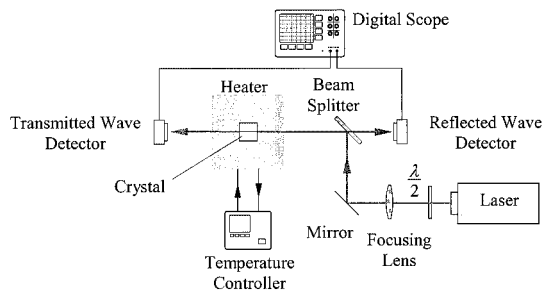


Fig. 1. Experimental setup for measuring the thermal-induced optical-path change in the crystal.

inside the crystal at different wavelengths and the measurement of the crystal thermal expansion.

In Section 2 we describe the experimental setup for measuring the temperature dependence of the refractive index and provide the measurement results. In Section 3 we derive the temperature dependence of the refractive indexes and discuss the application of the derived equation to experimental data of different nonlinear optics experiments. Finally, in Section 4 we summarize the main results of this work.

2. Experimental Setup

A 9.1-mm flux-grown KTP crystal and an 11.35-mm flux-grown KTA crystal were used in these measurements, and their input and output end faces were polished perpendicular to the x axis. The thickness of both crystals was 0.5 mm. Such crystal configuration enabled us to measure y and z components of the refractive index, using our technique. Note that the z component of the refractive index is the most relevant for quasi-phase-matched interactions in KTP and KTA, since the interacting waves are usually polarized in this direction.

We first interferometrically measured the optical path change as a function of temperature using the setup shown in Fig. 1. The laser light beam, with a waist of $\sim 150 \mu\text{m}$ at the middle of the crystal, propagated along the x axis, and its polarization was set either in the y or the z direction. For the measurement that was done at the 1509–1585 nm wavelength range, the polarization was controlled by an optic fiber polarization controller and polarizer, and for the measurements at all other wavelengths it was done by a half-wave plate. The crystal temperature was controlled in the range 25–200 °C by a heater and a temperature controller, with an accuracy of 0.1 °C. The heater was made from two parts. The outer part was the thermal insulator, made from two layers of Teflon, separated by a 5-mm air space. The inner part was made of copper and included a base element, containing two heaters and a temperature sensor, and a copper cover. The first version of the heater was made in so that both the top and the bottom sides of the crystal were in contact with the heater. Unfortunately strong temperature gradi-

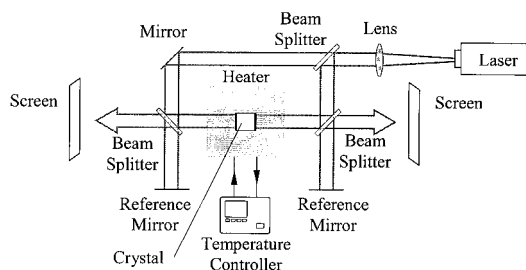


Fig. 2. Experimental setup for measuring the crystal thermal expansion.

ents inside the crystal in the z direction were observed during the heating. Therefore we modified the heater so that only the bottom side of the crystal was in direct contact with the copper while a 0.5-mm air space was left between the crystal top side and the heater cover. We compared two methods of mounting inside the heater; the crystal either simply was resting inside the heater or was placed on the thin layer of the thermal grease. However, we have not observed a significant difference between the two mounting methods.

The peak-to-peak change in the transmitted-wave intensity, as a function of temperature, was $\sim 25\%$ at room temperature, which is $\sim 5\%$ less than theoretical. This difference can be explained by internal crystal loss, relatively low quality of crystal end faces, and some other loss factors of the system. During the heating the peak-to-peak change in the transmitted-wave intensity was decreased, reaching the value of $\sim 15\%$, up to 200 °C. Such behavior can be explained by an increased temperature gradient inside the crystal in the z direction up to $\sim 1.3 \text{ }^\circ\text{C}/\text{mm}$. Neglecting the temperature gradient inside the copper body of the heater and taking into account the actual crystal thickness, the maximum difference between the detected heater temperature and the actual temperature in the middle of the crystal should be less than 0.7 °C for the worst case. It will be shown later in this paper that such an error factor is negligible, compared with other factors, in influencing the final result.

Several different commercial lasers at the following wavelengths were used as light sources: 532 nm (frequency-doubled Nd:YAG laser); 775 and 787 nm (external-cavity-diode laser); 1064 nm (Nd:YAG laser); and 1509, 1545, and 1585 nm (external-cavity-diode laser). All light sources emitted at a single transversal and longitudinal mode and their wavelengths were measured with an optical wavemeter with 1-pm accuracy. The measured phase change was found to have a nearly parabolic form, and the relative accuracy of parabolic fit coefficients for the measured data was $\sim 0.3\%$. The main factors that limited this accuracy were small temperature instability (up to 0.1 °C) and small variations of the laser wavelength during the measurement.

For the crystal thermal expansion measurement we used the experimental setup shown in Fig. 2.

Table 1. Thermal Expansion Coefficients of KTP and KTA

Material	α [$^{\circ}\text{C}^{-1}$]	β [$^{\circ}\text{C}^{-2}$]
KTP	$(6.7 \pm 0.7) \times 10^{-6}$	$(11 \pm 2) \times 10^{-9}$
KTA	$(7.6 \pm 0.6) \times 10^{-6}$	$(8.4 \pm 1.2) \times 10^{-9}$

The crystal end faces were chemically coated with a silver-based reflecting coating, so the reflection was increased up to 90–95% and transmission was decreased to practically zero. Two Twyman–Green interferometers were formed, where one of the mirrors of each interferometer was the reflecting crystal end face, and the other was a fixed reference mirror. The interfering beams from the two interferometers were measured with a 532-nm frequency-doubled Nd:YAG laser. The thermal expansion of the crystal displaced the crystal end faces relative to each reference mirror, thereby causing fringe displacement. Although this displacement was mainly due to crystal expansion, it included a small contribution, owing to the change of the air refractive index with temperature. To evaluate the contribution of the air heating, we measured the temperature profile of the air near the heater, and the corresponding optical path change was theoretically calculated.^{8,9} In addition, the optical path change was interferometrically measured through an empty heater after the crystal was removed. The results of these two methods differed by 20%. Taking into account the practical limitations of both methods, we took the average value between the two results. The uncertainty in estimating the contribution of air heating is the largest uncertainty in the experiment, and it yielded a 10% error on the crystal’s thermal expansion value.

The thermal expansion was found to be governed by parabolic dependence on temperature:

$$L = L_0[1 + \alpha(T - 25 \text{ }^{\circ}\text{C}) + \beta(T - 25 \text{ }^{\circ}\text{C})^2]. \quad (1)$$

The thermal expansion coefficients are given in Table 1. The value of linear thermal expansion coefficient α for KTP was previously reported¹⁰ as $8.7 \times 10^{-6} \text{ }^{\circ}\text{C}^{-1}$ at $T = 100 \text{ }^{\circ}\text{C}$. This value is in good agreement with the overall expansion of $(8.3 \pm 0.8) \times 10^{-6} \text{ }^{\circ}\text{C}^{-1}$, calculated with Eq. (1) and normalized linearly to the temperature change from room temperature to $100 \text{ }^{\circ}\text{C}$. For KTA our results are also in good agreement with values calculated from previ-

ously known data¹¹: $\alpha = 7.7 \times 10^{-6} \text{ }^{\circ}\text{C}^{-1}$, $\beta = 7.1 \times 10^{-9} \text{ }^{\circ}\text{C}^{-2}$.

3. Deriving the Temperature Dependence of the Refractive Index

Finally, the thermal expansion coefficients together with the measured optical path change measurements for all measured wavelengths were used to derive the refractive index change versus temperature. The known data for the refractive indexes of crystals at room temperature^{1–3,12} were used for this calculation: Ref. 1 for the z component of the KTP refractive index, Ref. 2 for the z component of the KTA refractive index, Ref. 3 for the y component of the KTA refractive index, and Ref. 12 for the y component of the KTP refractive index. It was found that Δn depends on temperature in a parabolic fashion:

$$\Delta n(\lambda, T) = n_1(\lambda)(T - 25 \text{ }^{\circ}\text{C}) + n_2(\lambda)(T - 25 \text{ }^{\circ}\text{C})^2. \quad (2)$$

The parabolic coefficients n_1 and n_2 can be expressed as the third-order polynomial of negative powers of wavelength (3):

$$n_{1,2}(\lambda) = \sum_{m=0}^3 \frac{a_m}{\lambda^m}. \quad (3)$$

(The wavelengths are given in micrometers.) The a_m coefficients for both crystals in y and z polarization are given in Table 2.

The derived equations were applied to other experimental data in order to verify our results. The first temperature derivatives $n_1(\lambda)$ were compared with the results of Wiechmann and Kubota⁵ and Kato and Takaoka⁷; see Fig. 3. There is a good agreement between our results and those in Refs. 5 and 7 at short wavelengths, up to 0.8 and 1.1 μm for the y and z directions, respectively. The deviations are more dominant at longer wavelengths. Note that the calculations in Ref. 5 were based on measurements up to 1.13 μm , whereas in this work the measurement wavelength range was extended to 1.58 μm . In addition, the parabolic factor n_2 will lead to additional differences at high temperatures, i.e., above $100 \text{ }^{\circ}\text{C}$. In a similar way, Fig. 4 shows the first temperature derivatives of KTA. Next, Eq. (3) was compared with temperature-tuned PPKTP OPO data^{4,13}; see Fig. 5. The fits calculated from Wiechmann and

Table 2. Temperature Dependence Fit Coefficients for KTP and KTA

	KTP				KTA			
	z-axis		y-axis		z-axis		y-axis	
	n_1 [10^{-6}]	n_2 [10^{-8}]	n_1 [10^{-6}]	n_2 [10^{-8}]	n_1 [10^{-6}]	n_2 [10^{-8}]	n_1 [10^{-6}]	n_2 [10^{-8}]
a_0	9.9587	-1.1882	6.2897	-0.14445	-6.1537	-0.96751	-4.1053	0.5857
a_1	9.9228	10.459	6.3061	2.2244	64.505	13.192	44.261	3.9386
a_2	-8.9603	-9.8136	-6.0629	-3.5770	-56.447	-11.78	-38.012	-4.0081
a_3	4.1010	3.1481	2.6486	1.3470	17.169	3.6292	11.302	1.4316

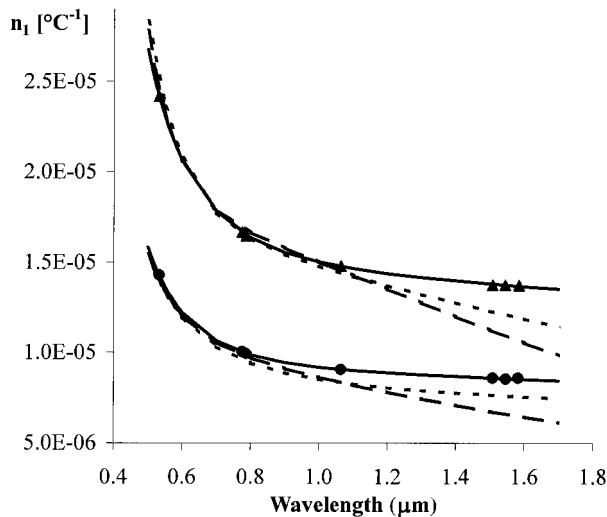


Fig. 3. First temperature derivative of the refractive index of KTP, n_1 , as a function of wavelength. \blacktriangle , z -axis measurements; \bullet , y -axis measurements; solid curves, theoretical fit from Eq. (3); long dashed curves, calculation from Ref. 5; short dashed curves, calculation using Ref. 12.

Kubota⁵ are not shown, since they are almost identical to those of Kato and Takaoka⁷: There is a slight difference only for the two first crystal periods at high temperatures, whereas the equation in Kato and Takaoka better fits the measurement data. The calculation based on Eq. (3) is in much better agreement with the experimental results than the previously available equations.^{5,7}

We also tested Eq. (3) at longer wavelengths in the mid-IR range near 3.5 μm , using experimental results of a PPKTP difference-frequency generator.¹ The thermal tuning slope in the mid-IR range was measured to be $-0.84 \text{ nm}/^\circ\text{C}$, as it appears from the raw data of Ref. 1. References 5 and 7 predict thermal tuning slopes of $-2.4 \text{ nm}/^\circ\text{C}$ and $-0.88 \text{ nm}/^\circ\text{C}$, respectively, whereas the calculated slope based on

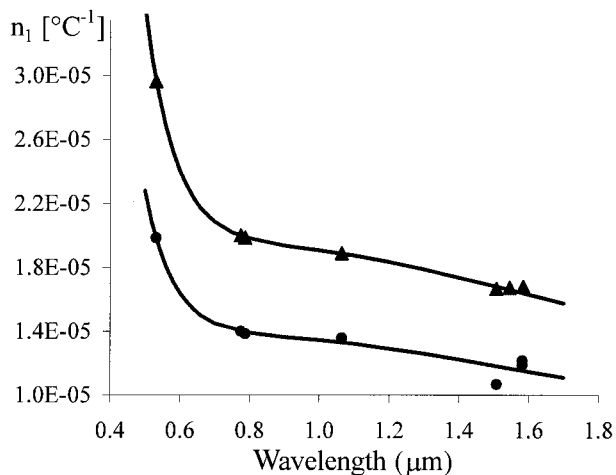


Fig. 4. First temperature derivative of the refractive index of KTA, n_1 , as a function of wavelength. \blacktriangle , z -axis measurements; \bullet , y -axis measurements; solid curves, theoretical fit from Eq. (3).

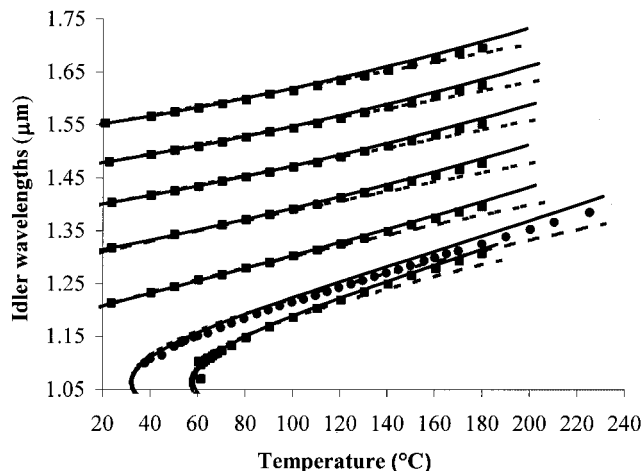


Fig. 5. Idler temperature tuning slopes of PPKTP optical parametric oscillator. \bullet , experimental results from Ref. 4; \blacksquare , experimental results from Ref. 13; solid curves, calculation from Eq. (3); short dashed curves, calculation from Ref. 12.

Eq. (3) is $-0.68 \text{ nm}/^\circ\text{C}$, which is fairly close to the measured value. The measured FWHM¹ is $\sim 70^\circ$. The values calculated from Refs. 5 and 7 are 14° and 39° , respectively, whereas Eq. (3) predicts a FWHM of 54° . For these calculations we took into account the linear term of the thermal expansion from Table 1. Hence, although our measurements were taken up to only 1.58 μm , Equation (3) provides the dependence of the refractive index on the temperature with reasonable accuracy at much longer wavelengths.

We also compared the equation for KTA temperature-dependent refractive index with difference frequency generator measurement results.² The temperature tuning slope calculated from Eq. (3) was found to be $-2.4 \text{ nm}/^\circ\text{C}$, which differs from the measured value of $-0.94 \text{ nm}/^\circ\text{C}$. The calculated value of the temperature FWHM calculated from Eq. (3) is 19° , which does not agree with the measured value of 62° . Hence it seems that unlike KTP, the predictions for KTA in the mid-IR range, based on measurements in the visible and near-IR ranges, are not accurate enough. To improve the accuracy at long wavelengths, we have used the measurement results for temperature-tuned KTA OPO¹⁴ together with our results at 1.55 μm . We found that a correction term should be added to Eq. (3):

$$n_{1,2(\lambda)} = \sum_{m=0}^3 \frac{a_m}{\lambda^m} + \frac{B(\lambda - \lambda_0)}{1 + \exp[-\gamma(\lambda - \lambda_0)]}, \quad (4)$$

where $\lambda_0 = 1.55$ and $\gamma = 10 \mu\text{m}^{-1}$, respectively, for both n_1 and n_2 , and $B = (4.6 \pm 1.0) \times 10^{-6} [\mu\text{m}^{-1} \text{ } ^\circ\text{C}^{-1}]$ and $(8 \pm 5) \times 10^{-9} [\mu\text{m}^{-1} \times \text{ } ^\circ\text{C}^{-2}]$ for n_1 and n_2 , respectively. This correction is constructed in such a form that it becomes significant for wavelengths longer than 1.55 μm and fits the values of n_1 and n_2 pass to the data of Ref. 14. Since the measurements of Ref. 14 were done for the z component of the refractive index, the correction term was developed only for this component.

The values of temperature tuning slope and the FWHM of the difference frequency generator,² calculated from Eq. (4), are $-1.14 \text{ nm}/^\circ\text{C}$ and 42° , respectively, which are much closer to the measured values.

It should be noted that in order to fit the experimental results of the PPKTP OPO,^{4,13} a fixed temperature shift of $\sim 25^\circ\text{C}$ had to be introduced. This temperature shift is equivalent to a linear change of the wave-vector mismatch value: $\Delta k = 4800 - 210 \Lambda$. (Λ is the crystal poling period, given in micrometers, and Δk units are inverse meters.) Furthermore, by observing several measurements at different periods and temperatures,¹⁵ we have found that this correction factor also changes with temperature, with a slope of $\sim 22 \text{ m}^{-1}$ per degree (calculated from a wavelength tuning of the second-harmonic peak for two crystal periods; see Ref. 15). The origin of this behavior is not completely understood, and further research is required. Fortunately, the shift of the wave-vector mismatch value has no effect on the derivation of the temperature dependence of the refractive index.

4. Summary

We have performed measurements of the temperature dependence of the refractive index of KTP and KTA over a wide temperature and wavelength range. We have found that both the refractive index change and the thermal expansion have a parabolic dependence on the temperature. These measurements provided temperature-dependent Sellmeier equations with improved accuracy for these two materials. In KTP, the main improvements are at temperatures above 100°C and at wavelengths above $1 \mu\text{m}$. As for KTA, we believe that this is the first time that the temperature dependence of the refractive index is reported. These equations are in good agreement with previously published experimental results and are useful for designing temperature-tuned nonlinear frequency converters in the visible, near-IR, and mid-IR ranges.

References

1. K. Fradkin, A. Arie, A. Skliar, and G. Rosenman, "Tunable midinfrared source by difference frequency generation in bulk

- periodically poled KTiOPO_4 ," *Appl. Phys. Lett.* **74**, 914–916 (1999).
2. K. Fradkin-Kashi, A. Arie, P. Urenski, and G. Rosenman, "Mid-infrared difference-frequency generation in periodically poled KTiOAsO_4 and application to gas sensing," *Opt. Lett.* **25**, 743–745 (2000).
3. D. L. Fenimore, K. L. Schepler, U. B. Ramabadran, and S. R. McPherson, "Infrared corrected Sellmeier coefficients for potassium titanyl arsenate," *J. Opt. Soc. Am. B* **12**, 794–796 (1995).
4. D. R. Wiese, U. Stroessner, A. Peters, J. Mlynek, S. Schiller, A. Arie, A. Skliar, and G. Rosenman, "Continuous-wave 532-nm-pumped singly resonant optical parametric oscillator with periodically poled KTiOPO_4 ," *Opt. Commun.* **184**, 329–333 (2000).
5. W. Wiechmann and S. Kubota, "Refractive-index temperature derivatives of potassium titanyl phosphate," *Opt. Lett.* **18**, 1208–1210 (1993).
6. K. Kato, "Temperature insensitive SHG at $0.5321 \mu\text{m}$ in KTP," *IEEE J. Quantum Electron.* **28**, 1974–1976 (1992).
7. K. Kato and E. Takaoka, "Sellmeier and thermo-optic formulas for KTP," *Appl. Opt.* **41**, 5040–5044 (2002).
8. H. Fang and P. Juncar, "A new simple compact refractometer applied to measurements of air density fluctuations," *Rev. Sci. Instrum.* **70**, 3160–3166 (1999).
9. B. Edlen, "The dispersion of standard air," *J. Opt. Soc. Am.* **43**, 339–344 (1953).
10. Almaz Optics, Inc., 12 Chadsford Court, Marlton, N.J., <http://www.almazoptics.com/homepage/KTP.htm>.
11. Z. Zhong, P. K. Gallagher, D. L. Loiacono, and G. M. Loiacono, "The thermal expansion and stability of KTiOAsO_4 and related compounds," *Thermo. Chim. Acta* **234**, 255–261 (1994).
12. T. Y. Fan, C. E. Huang, B. Q. Hu, R. C. Eckardt, Y. X. Fan, R. L. Byer, and R. S. Feigelson, "Second harmonic generation and accurate index of refraction measurement in flux-grown KTiOPO_4 ," *Appl. Opt.* **26**, 2390–2394 (1987).
13. U. Strossner, J. P. Meyn, R. Wallenstein, P. Urenski, A. Arie, G. Rosenman, J. Mlynek, S. Schiller, and A. Peters, "Single-frequency continuous-wave optical parametric oscillator system with an ultrawide tuning range of 550 to 2830 nm," *J. Opt. Soc. Am. B* **19**, 1419–1424 (2002).
14. Y. Findlyng, "Periodical poling of KTiOAsO_4 crystals for nonlinear optical applications," M.Sc. thesis (Faculty of Engineering, Tel-Aviv University, Tel-Aviv, Israel, 1998).
15. A. Arie, G. Rosenman, V. Mahal, A. Skliar, M. Oron, M. Katz, and D. Eger, "Green and ultraviolet quasi-phase-matched second harmonic generation in bulk periodically-poled KTiOPO_4 ," *Opt. Commun.* **142**, 265–268 (1997).